Femtosecond Laser Ionization Mass Spectrometry for Online Analysis of Human Exhaled Breath

Yoshinaga, Katsunori
Faculty of Design, Kyushu University

Imasaka, Totaro
Kyushu University

Imasaka, Tomoko
Faculty of Design, Kyushu University

出版情報：Analytical Chemistry. 96 (28), pp.11542-11548, 2024-07-07. American Chemical Society (ACS)
バージョン：

Femtosecond Laser Ionization Mass Spectrometry for Online Analysis of Human Exhaled Breath

Katsunori Yoshinaga,[a] Totaro Imasaka,[b,c] and Tomoko Imasaka[a,*]

[a]*Faculty of Design, Kyushu University, 4-9-1, Shiobaru, Minami-ku, Fukuoka 815-8540: 744 Motooka, Nishi-ku, Fukuoka 819-0395, Japan*

[b]*Kyushu University, 744 Motooka, Nishi-ku, Fukuoka 819-0395, Japan*

[c]*Hikari Giken, Co., 2-10-30, Sakurazaka, Chuou-ku, Fukuoka 810-0024, Japan*

* Corresponding author:

Email address: imasaka@design.kyushu-u.ac.jp (Tomoko Imasaka)

ABSTRACT: A variety of organic compounds in human exhaled breath were measured online by mass spectrometry using the fifth (206 nm) and fourth (257 nm) harmonic emissions of a femtosecond ytterbium (Yb) laser as the ionization source. Molecular ions were enhanced significantly by means of resonance-enhanced, two-color, two-photon ionization, which was useful for discrimination of analytes against the background. The limit of detection was 0.15 ppm for acetone in air. The concentration of acetone in exhaled breath was determined for three subjects to average 0.31 ppm, which lies within the range of normal healthy subjects and is appreciably lower than the range for patients with diabetes mellitus. Many other constituents, which could be assigned to acetaldehyde, ethanol, isoprene, phenol, octane, ethyl butanoate, indole, octanol, etc., were observed in the exhaled air. Therefore, the present approach shows potential for use in the online analysis of diabetes mellitus and also for the diagnosis of various diseases such as COVID-19 and cancers.

■ INTRODUCTION

Obesity and diabetes are serious concerns in modern society. In fact, more than 500 million people are reported to have become patients of diabetes in 2021, which corresponds to 10 percent of adults in the world.[1] This number is expected to increase in the future, and new technology must be developed to meet the coming demand for diagnoses. It is common knowledge that diabetes is caused by insufficient or reduced capacity for insulin as are referred to as Type 1 (genetic defect) and Type 2 (lifestyle disease). If the presence of insulin is improper, carbohydrates in blood cannot pass through cell membranes. When this hyperglycemic state continues, people develop diabetes mellitus since the concentration of the carbohydrate can no longer be controlled by insulin. The degree of diabetes could be evaluated from the amount of glucose bound to hemoglobin in the blood, the parameter of which is referred to as Hemoglobin A1c (HbA1c). This method is, however, invasive and places a heavy physical burden on the patient. When biological energy is needed during the hypoglycemic state, fat is then metabolized. Ketone bodies such as acetone are produced and the blood becomes acidic, which results in a condition that is referred to as "ketoacidosis". Acetone contained in the blood is released from the alveoli into the exhaled air, so that the concentration of acetone in the breath gas increases. Accordingly, the degree of diabetes could be evaluated by measuring the concentration of acetone. On the other hand, the exhaled gas contains numerous chemical species such as isoprene that are used as biomarkers of oxidative stress.[2,3] Note that there were 20 million new cancer cases and 9.7 million deaths in 2022 and that approximately 1 in 9 men and 1 in 12 women die from cancers each year.[4] Several trace gases in exhaled breath are used as biomarkers for stomach, lung, breast, colorectal, and other cancers.[5] Therefore, valuable information about human health and pathophysiology could be obtained by measuring the trace gases in exhaled air.

There are several analytical techniques for determining the constituents in breath gas.[6] For example, a semiconductor sensor has been developed to monitor the concentration of a trace gas in exhaled breath. Advantages of the semiconductor device are small size, low cost, and a short response time. This type of sensor is preferential for portable and personal use in monitoring health conditions. Many types of semiconductor materials have been studied to improve selectivity. For example, Si-doped WO_3 nanoparticles,[7] Au and Pd nanoparticle-decorated WO_3 nanorods,[8] In_2O_3 sensors layer-by-layer-coated with CeO_2 nanoclusters,[9] nanoscale PdO catalyst-functionalized CO_3O_4 hollow nanocages,[10] have been developed for measuring acetone. To improve selectivity, a sensor is combined with a separation channel,[11] which permits the simultaneous online analysis of several compounds. Such a semiconductor device is already commercially available. One of the major problems associated with the semiconductor sensor is the difficulty in predicting the effect of interference, since the response mechanism is not necessarily clear. Another approach is to use the enzymatic reaction of nicotinamide adenine dinucleotide (NADH $\leftrightarrow NAD^+$) with alcohol dehydrogenase.[12-15] In this method, exhaled gas is introduced into a flow cell with the enzyme immobilized onto a fiber-optic sensor, in which NADH is excited at 340 nm using a light-emitting diode and the fluorescence is measured at 490 nm using a photomultiplier. Using this method, acetone, isopropanol, or acetaldehyde in exhaled breath, as well as ethanol on the skin, is determined at ppb levels.

For multi-component analysis, exhaled air has been measured via gas chromatography combined with electron ionization mass spectrometry (GC/EI-MS).[5,6,16] For preparation of the sample, analytes are adsorbed onto a fiber for solid-phase microextraction (SPME),

which is followed by GC/EI-MS.[17-19] Numerous organic compounds have been determined at ppb levels. A comprehensive two-dimensional technique based on GC and time-of-flight mass spectrometry (TOFMS) is employed for monitoring 60 compounds in breath gas derived from a patient following the induction of anesthesia.[20,21] This approach is sensitive and even allows the differentiation of isomers. However, it takes much time to condition the tools and devices such as a sampling bag and a fiber for SPME, which then must be followed by lengthy GC analysis.

For the online analysis of exhaled air, GC should be removed before MS is conducted. It is, however, difficult to use EI-MS for this purpose, since the filament used for EI is deteriorated by O_2 in the air. For this reason, a different type of ionization technique must be developed for trace analysis of the constituents in exhaled breath. A method that is referred to as proton-transfer-reaction mass spectrometry (PTR-MS), has been developed to solve this problem,[22,23] in which H_2O is first ionized by a corona discharge to produce H_3O^+ and the positive charge (H^+) is transferred to an analyte molecule when the proton affinity is larger than the value of H_2O (691 kJ mol-1).[22] Aromatic hydrocarbons such as toluene, conjugated aliphatic compounds such as isoprene, and oxygen-containing compounds such as acetone are determined even in the presence of large amounts of ambient N_2 and O_2 because of their small proton affinities. Due to the small amount of excess energy remaining in the ions, the fragmentation is markedly suppressed, which provides a mass spectrum that is simpler than that of EI-MS. This type of analytical instrument is already commercially available and has been utilized in various applications.[24,25] For further improvement in selectivity, the instrument is combined with GC in a series and also in parallel.[26-28] In PTR-MS, numerous ionic species such as $H_3O(H_2O)_n^+$ are used as primary (precursor, reactant, or reagent) ions. To simplify the mass spectrum, an ion such as H_3O^+ that is produced by microwave discharge is isolated using a first mass filter (mass spectrometer). This ion then serves as the source for ionization by charge transfer reaction in a buffer gas of He at reduced pressure, which is followed by mass analysis using a second mass spectrometer, as is referred to as selected ion flow tube mass spectrometry (SIFT-MS).[3,29] The advantages of PTR-MS and SIFT-MS include high sensitivity (ppb levels) and the suppression of major signals arising from ambient N_2 and O_2, although the analytical instrument is bulky (complicated) and requires a trained operator.[6]

Photoionization mass spectrometry has been developed to simplify mass spectra. A technique of single-photon ionization mass spectrometry (SPI-MS) is already being utilized to measure breath gas. For example, a pulsed-electron-beam-pumped excimer lamp containing an argon gas is used to produce vacuum-ultraviolet (VUV) emissions (9.8 ± 0.4 eV, 126 ± 9 nm) and is employed as the ionization source.[30] Acetone, isoprene, and phenol in exhaled breath are measured for a normal subject, i.e., a non-smoker. A combination with GC allows a selective determination of isomers.[31] On the other hand, aromatic hydrocarbons such as phenol and indole have been measured by multiphoton ionization mass spectrometry (MPI-MS) using a tunable nanosecond laser as the ionization source.[31] Nitric oxide (NO) in exhaled gas is determined by MPI-MS at ppb levels.[32] Recently, femtosecond laser ionization mass spectrometry (fs-LIMS) has been developed for trace analysis of various organic compounds.[33-36] For example, the aromatic and aliphatic compounds of environmental pollutants such as dioxins and pesticides, explosives such as triacetone triperoxide, and psychological substances such as barbiturates are measured using an ultraviolet femtosecond optical pulse produced

using the harmonic generation of a T:sapphire laser (800 nm) as the ionization source, which permits actual trace analysis when combined with GC. On the other hand, nitro polycyclic aromatic hydrocarbons such as the nitropyrene in particulate matter 2.5 (PM2.5) that is obtained from diesel exhaust gas have been determined based on two-color, two-photon ionization using the third (343 nm) and fourth (257 m) harmonic emissions of an ytterbium (Yb) laser (1030 nm).[37] More recently, the fatty acid methyl esters in biofuel were measured using the fourth (257 nm) and fifth (206 nm) harmonic emissions as the ionization source.[38]

In the present study, we developed an analytical instrument based on fs-LIMS for the online real-time analysis of the constituents in human exhaled breath. With this system, a two-color ionization scheme (257 and 206 nm) was employed to increase the signal intensity of the molecular ions by means of resonance-enhanced two-photon ionization. We applied fs-LIMS to an online analysis of exhaled gas from three subjects. As a result, various organic compounds such as acetone, isoprene, and acetaldehyde were simultaneously observed in the mass spectra. The potential advantages of using fs-LIMS in place of either PTR-MS or SIFT-MS are discussed for use in the online analysis of diabetes mellitus and also in the diagnoses of various diseases such as COVID-19 and cancers.

■ EXPERIMENTAL SECTION

Analytical instrument. A block diagram of the experimental apparatus is shown in Fig. 1. The operation principle and the details of the instrument are reported elsewhere.[39] Briefly, a sample is introduced through a narrow fused-silica capillary (i.d., 0.25 mm; length, 10 m) into a small-frame mass analyzer (typical flow rate, 1 mL/min) consisting of a short flight tube (length, 65 mm) and a small vacuum chamber (width, 200 mm; length, 160 mm; height, 130 mm), and the sample is then evacuated using a small turbo molecular pump (150 L/s) followed by a rotary pump (60 L/min). Ions are detected using an assembly of microchannel plates (response time, 600 ps). A mass spectrum was constructed via time-correlated single-ion counting, in which the signal of laser pulses served as the start pulse and the signal of single-ion pulses from the microchannel plate detector served as the stop pulse. The time interval between the start and stop pulses was measured using a time-to-digital converter (time resolution, 250 ps). The accumulation time of the signal was 120 s in this study to construct a histogram, i.e., mass spectrum, using a software program developed in this laboratory. A femtosecond Yb laser (repetition rate, 120 kHz; wavelength, 1030 nm; pulse width, 400 fs) was employed as a fundamental beam to generate harmonic emissions using a series of nonlinear optical crystals (β-$BaBO_3$) (the photograph is shown in Fig. S1 in the Supporting Information). The fourth harmonic emission (257 nm) and the fifth harmonic emission (206 nm) were separated and then recombined using dichroic mirrors to adjust the timing of the two pulses. The separation of the pulses was set at $\Delta t = 0$ in this study by translating the stage mounting the mirrors using a micrometer head (see the photograph in Fig. S1). The two laser beams were focused together using a concave mirror with a focal length of 20 cm, the diameter, the fluence, the peak power, and the intensity at the focal point for FHG (FIHG) being estimated to be 3.3 (2.6) μm, 6.2 (2.9) J/cm^2, 3.4 (1.1) GW, and 4.1 (2.0) × 10^{13} W/cm^2, respectively.

Samples. A standard gas of acetone was prepared using a commercially available

permeator (Gas Tech, PD-1B). The concentration was adjusted by changing the temperature of the diffusion tube and the flow rate of the synthesized pure air (N_2, 78.5-80%; O_2, 20-21.5%; CO, <1 ppm; CO_2, <2 ppm; CH_4, <3 ppm; H_2O, <10 ppm) supplied from a gas cylinder (Iwatani Co.). No standard gas of isoprene was prepared since no data of physical parameters were available in the list of the manufacturer's manual. The exhaled gas of human breath was sampled from the three authors of this study. Ambient laboratory air was directly introduced to the mass analyzer without a filter to measure the background signal. Acetone reagent was purchased from Sigma-Aldrich Co.

■ RESULTS AND DISCUSSION

Ionization scheme. The absorption spectrum of acetone, reported in the database of the National Institute of Standards and Technology (NIST), consists of a broad-band structure ($\log \varepsilon > 3.2$) in the spectral region of 220-300 nm with an absorption maximum ($\log \varepsilon = 4.25$) at 266 nm ($\log \varepsilon = 4.20$ at 257 nm).[40] This absorption band is assigned to the $\pi^* \leftarrow$ n transition of the C=O bond.[41] The database lists the ionization energy (*IE*) of acetone at 9.703 ± 0.0006 eV (the ionization scheme of acetone at different wavelengths are summarized in Fig. S2).[40] The two-photon energy (9.63 eV) of the fourth harmonic emission (257 nm) is slightly smaller than the ionization energy, which meant three photons were required for ionization, and this resulted in a large excess of energy at 4.74 eV. On the other hand, it was possible to ionize acetone using two photons (12.04 eV) at 206 nm, which reduced the excess energy to 2.33 eV. The excess energy could be further reduced to 1.13 eV using two photons (10.83 eV) at 257 and 206 nm in a process referred to as resonance-enhanced, two-color, two-photon ionization. Actually, the molecular ion was significantly enhanced and the fragmentation was suppressed by using this scheme (see the mass spectra obtained at different laser wavelengths shown in Fig. S3 and the explanation (text) in the Supporting Information). Major constituents in the air such as N_2, O_2, H_2O, and CO_2 are less efficiently ionized by comparison with organic compounds such as acetone, since more than three photons are required for these inorganic compounds even at 206 nm (the ionization schemes are shown in Fig. S6). This selectivity is necessary due to a limited dynamic range of the mass spectrometer (ca. 10^5), since the concentrations of these major constituents in the air are $>10^6$-fold larger than the analytes in the exhaled gas.

Determination of acetone in the air. A mass spectrum was measured for a sample containing acetone that was diluted at 10 ppm with synthesized pure air. The result is shown in Fig. 2 (A), along with the mass spectrum obtained for the pure air to measure the background as shown in Fig. 2 (B) (the data displayed at a reduced scale appear in Fig. S7). Many signal peaks arising from the constituents in the air such as N_2, O_2, and H_2O (<10 ppm) appeared in the mass spectrum measured for the background. The ratio of the signal intensities for the peaks observed at m/z = 34 and 32 was 0.0018, which reasonably agreed with an isotope abundance ratio of 0.0020 for ^{18}O and ^{16}O. Then, the signal at m/z = 34 could be assigned to the isotopomer, $[^{16}O^{18}O]^+$, of $[^{16}O_2]^+$. When acetone was introduced into the mass spectrometer, the molecular ion $[M]^+$ was clearly observed at m/z = 58 in addition to the isotopomer ion of $^{13}C^{12}C_2H_6O$ at m/z = 59 and the fragment ions, $[M-1]^+$ and $[M-15]^+$, at m/z = 57 and 43, respectively. Broad background signals were observed in the m/z regions that were larger than those of either N^+ and O^+ (m/z = 14 and 16) or N_2^+ and O_2^+ (m/z = 28 and 32). Accordingly, in order to minimize

the background, molecular ions that are observable at larger m/z values are more suitable than the fragment ions observed at smaller m/z values. Such broad signals were suspected to arise from N^+/O^+ and N_2^+/O_2^+, the flight time of which was slightly increased by a collision or a charge transfer reaction with ambient N_2 and O_2 introduced into the mass analyzer. In fact, the background signals drastically decreased with a decrease in the vacuum pressure of the chamber, although the signal intensity of acetone also decreased. In the present study, the background pressure was optimized at 10^{-2} Pa so as to increase the signal intensity of acetone and to minimize the background signal. A vacuum pump with a larger capacity would be preferential for background suppression.

The limit of detection (LOD) was measured at 0.15 ppm for acetone from the signal intensity of the molecular ion observed at *m/z* = 58 and the variation in the background signal. Note that the LOD was increased significantly by a large excess energy (1.13 eV) and more dissociative nature of acetone due to an active site of C=O. This value was lower than the 0.22 - 0.80 ppm and 1.76 - 3.73 ppm figures reported for healthy subjects and diabetes mellitus, respectively, as measured by GC-MS,[17] and also was lower than the 0.2 - 0.6 ppm reported for healthy subjects measured by SIFT-MS.[2] Thus, the analytical instrument developed in this study had sufficient sensitivity for the online analysis of acetone in exhaled breath. A linear analytical curve was constructed in a range of from 0 to 100 ppm (the data appear in Fig. S8).

Analysis of human breath: Isoprene. The mass spectra measured for the exhaled breath of one of the three subjects and for the ambient air in the laboratory appear in Fig. 3, and show the various chemical species present in human breath. A molecular ion, $[CH_2=C(CH_3)CH=CH_2]^+$, of isoprene was clearly observed at *m/z* = 68 (the data displayed at a reduced scale for the three subjects appear in Fig. S9) in addition to an isotopomer, $[^{12}C_4{}^{13}CH_8]^+$, observed at *m/z* = 69. Several fragment ions, $[CH_2=C(CH_3)C=CH_2]^+$, $[CH_2=C\text{-}CH=CH_2]^+$, $[C_3H_5]^+$, $[C_3H_4]^+$, and $[C_3H_3]^+$, also appeared at *m/z* = 67, 53, 41, 40, and 39, respectively, which is consistent with the NIST EI-MS database.[40] Note that the signal at *m/z* = 68 cannot be assigned to furan (C_4H_4O, *m/z* = 68), which is an isobaric compound of isoprene, since fragment ions are seldom observed at *m/z* = 67, 53, and 41 for furan in the NIST EI-MS database.[40] The concentration level of isoprene in human breath is reported to be 5.8 - 274.9 ppb and ca. 100 ppb when measured using PTR-MS.[42,43] Accordingly, fs-LIMS has sufficient sensitivity for measuring isoprene in human breath at ppb levels. The concentration of isoprene, which is reported to increase with increases in both psychological and oxidative stress,[2] was compared among the three subjects (the data appear in Fig. S9). It is interesting to note that the concentration for one subject (a faculty member with educational responsibility) was 1.5 times higher than the others. Alternatively, a unique idea would be to monitor the concentration of isoprene in exhaled breath during cardiovascular surgery, since it increases drastically at the onset of physical exercise.[43] Due to a smaller flow rate for a sample in fs-LIMS (1 mL/min) than that in PTR-MS (100 mL/min), the present technique would be preferable for use in monitoring the biological gas emitted from smaller organisms. For example, PTR-MS has been utilized for the breath analysis of small animals such as frogs and snakes.[44] Therefore, fs-LIMS would be preferential for monitoring the gas emitted from tiny insects and even that from small plants as well.

Analysis of human breath: Acetone. A mass spectrum was measured three times for each of the three subjects (the data are shown in Fig. S10). The concentrations

of acetone were determined to be 0.30 ± 0.03, 0.34 ± 0.04, and 0.30 ± 0.02 ppm, respectively. These values were slightly larger than the background level observed for room air (0.15 ppm). The concentration level for a healthy subject is reported to be in the range of 0.2 - 0.8 ppm,[2,17] which suggests the possibility that obesity could be excluded for these subjects. In fact, the HbA1c values measured for the two subjects in a medical checkup were 5.3 and 5.6, and the normal range for HbA1c is <5.5 for a healthy subject. Therefore, the results obtained in this study are consistent with the values established for HbA1c, which suggests that a technique using fs-LIMS could be useful for the evaluations of obesity and diabetes mellitus.

Analysis of human breath: Other constituents. A large signal observed at *m/z* = 44 was assigned to the molecular ion, $[CH_3CHO]^+$, of acetaldehyde (*IE* = 10.229 ± 0.0007 eV), which is efficiently produced via weakly resonant (log ε = 0.7 at 257 nm), two-color, two-photon ionization (10.83 eV).[40] An assignment of this signal to CO_2^+ (*m/z* = 44) would be excluded, since CO_2 has a large ionization energy (13.777 ± 0.0001 eV)[40] and would appear through inefficient non-resonant three-photons ionization (14.45 eV) at 257 nm (the ionization scheme is shown in Fig. S6(D)). A small signal observed at *m/z* = 46 was assigned to the molecular ion, $[CH_3CH_2OH]^+$, of ethanol (*IE* = 10.48 ± 0.07 eV) produced by non-resonant, two-color, two-photon ionization.[40] As mentioned, an electron-beam-pumped argon excimer light source (9.8 ± 0.4 eV) was used for the single-photon ionization of a few organic compounds such as acetone in exhaled gas.[30] However, acetaldehyde and ethanol each have a larger level of ionization energy compared with that of single-photon energy and provide small ionization cross sections.[31] In fact, acetaldehyde was ionized using a VUV emission at 118 nm (10.49 eV) produced by the third harmonic generation of the third harmonic emission (355 nm) of a Nd:YAG laser (1064 nm) in Xe gas, where the analytes in the breath gas were collected using a Tedolar bag and were concentrated by a technique that involved needle-trap sampling and thermal-desorption.[45] This approach allows the determination of several aliphatic compounds such as acetone, acetaldehyde, isoprene, and cysteamine. In fs-LIMS, many chemical species have been observed in the mass range of *m/z* = 60 - 140, as shown in Fig. 4 (the data for the three subjects appear in Fig. S11), and are assigned to pentanol (88), phenol (94), ethylbenzene or xylene (106), octene (112), heptanal (114), ethyl butanoate (116), indole (117), and octanol (128), etc., for normal subjects. The signal of heptanal, which is suspected to be a biomarker for breast cancer,[46] was small and did not differ appreciably by gender. It should be noted that the signals observed at *m/z* = 18 increased drastically by comparison with the data obtained using pure air supplied from a gas cylinder. This result suggests that H_2O (*IE* = 12.621 ± 0.002 eV) appeared via inefficient three-photon ionization due to high concentrations of water in the samples of exhaled and room air.[40]

Comparison with PTR-MS and SIFT-MS: Enhancement of molecular ions. PTR-MS and SIFT-MS are advanced techniques for analyzing exhaled gas since they provide (quasi-)molecular ions as major signals, although large signals arising from precursor ions such as H_3O^+, $H_3O(H_2O)_n^+$, and others appear in the mass spectrum.[3] On the other hand, fs-LIMS provides a simpler mass spectrum since molecular ions and large fragment ions are observed in most cases, which makes the identification of analyte molecules easier even for a sample in a complex matrix. For example, a molecular ion was clearly observed as a major ion for isoprene in the present study (see Figs. 3(A) and

S8). The ratios of the signal intensities for the largest two fragment ions (*m/z* = 67 and 53) and the molecular ion (*m/z* = 68) were 0.63 and 0.02, respectively, in fs-LIMS. These values were smaller than the values of 1.54 and 0.98 reported in the EI-MS database.[40] In addition, the ratios for the largest two fragment ions (*m/z* = 41 and 39) and the quasi-molecular ion (*m/z* = 69) were reported to be 0.89 and 0.23, respectively, in PTR-MS.[42] Thus, fs-LIMS is preferential in terms of observing a molecular ion and large fragment ions, which provides valuable information concerning the molecular weight and the chemical structure of an analyte.

Comparison with PTR-MS and SIFT-MS: Selectivity switching. The ionization energy of isoprene is reported to be 8.86 eV ± 0.02 eV,[40] which means the excess energy remaining in the ionic state could be calculated to be 0.77 eV for single-color, two-photon ionization at 257 nm (9.63 eV). This value is smaller than the value of 1.97 eV achieved for two-color, two-photon ionization at 206 and 257 nm (10.83 eV). In the present study, single-color, two-photon ionization would be a major process, because of the pulse energy at 257 nm that is larger than that at 206 nm. Accordingly, the favorable result (suppression of fragmentation) achieved by fs-LIMS could be attributed to a level of excess energy (0.77 eV) that is smaller than the 1.46 eV achieved by PTR-MS that was calculated from the difference in the proton affinities of isoprene (198.9 kcal/mol, 8.63 eV) and H_2O (165.2 kcal/mol, 7.17 eV).[22] In PTR-MS, the primary reagent gas, which is H_2O, could be replaced with a different chemical such as either xylene (190.0 kcal/mol, 8.25 eV) or ethanol (185.6 kcal/mol, 8.06 eV) for the suppression of fragmentation,[22] although expertise for handling chemicals is required and compounds with smaller proton affinities become more difficult to ionize via proton transfer reaction. In fs-LIMS, the two-photon (or three-photon) energy could be switched instantly by interrupting one of the beams emitting at 206 or 257 nm. This approach is also useful for other combinations such as the fourth (257 nm) and the third (343 nm) harmonic emissions with a digit of 1.20 eV that corresponds to the one-photon energy of a Yb laser (1,030 nm).[37] For example, a molecular ion of heptanal (*IE* = 9.65 ± 0.02 eV), which is suspected to be a breast cancer biomarker,[40] could be determined more clearly by interrupting the fifth harmonic beam for single-color, two-photon ionization (9.63 ± 0.02 eV) at 257 nm.

Comparison with PTR-MS and SIFT-MS: Detection of inorganic compounds. In PTR-MS, it is difficult to measure chemical species with proton affinities that are smaller than that of H_2O. This is true for inorganic compounds such as N_2, O_2, and CO_2, alkanes such as methane and ethane, and some alkene/alkynes such as ethene/acetylene.[22,23] To measure such compounds, the primary reagent gas (H_2O) can be replaced with a different gas such as Kr (101.5 kcal/mol, 4.41 eV).[22,23] However, very large signals would appear for such inorganic compounds because of their high concentrations in the air, and the analytes with large proton affinities such as organic compounds would become more dissociative. Moreover, another high-pressure gas cylinder is needed, in addition to a cylinder for a buffer gas (He), which would require a license for transportation and installation. This situation is not an issue when using fs-LIMS, which does not require the use of high-pressure gas cylinders. The concentrations of H_2O, in addition to N_2 and O_2, could be determined by fs-LIMS, the sensitivity of which can be suppressed via an inefficient process of ionization. These types of signals can be used for normalization of the signals arising from the analytes. Alternatively, $^{18}O^{16}O$ or $^{18}O_2$, an isotopomer of $^{16}O_2$, could serve as a probe for biomedical studies.

Future applications: COVID-19 and influenza. Recently, PTR-MS has been utilized to measure COVID-19 biomarkers in human breath (accuracy, 97.3%).[47] A variety of chemical species are found in exhaled gas, among which NO and acetaldehyde are the first and second most important compounds, respectively. However, NO cannot be measured accurately using PTR-MS, since the ion is generated within the instrument by ionizing the surrounding air to produce a primary ion. This is probably due to the proton affinity of NO (127.1 kcal/mol, 5.52 eV),[40] which is smaller than that of H_2O (165.2 kcal/mol, 7.17 eV) and results in a difficult proton transfer reaction from H_3O^+. On the other hand, NO can be efficiently ionized via fs-LIMS, because the ionization energy (9.2642 ± 0.00002 eV) is slightly smaller than the two-photon energy (9.63 eV) of the fourth harmonic emission (257 nm).[40] Alternatively, the amount of acetaldehyde in human breath is known to increase by more than 75% in the case of COVID-19-positive patients and is also identified as a biomarker for Influenza A infections. [47,48] However, CO_2, an isobaric compound of acetaldehyde, accounts for an estimated 68% of the signal while the remainder is acetaldehyde in PTR-MS. Thus, the interference of CO_2 is crucial in PTR-MS. As we have previously established, however, such interference would be minimal in fs-LIMS because acetaldehyde is more efficiently ionized via weakly resonant, two-color, two-photon ionization than CO_2 ionized via non-resonant three-photon ionization at 257 nm.

Future applications: Cancers. The constituents in human exhaled breath have been measured by PTR-MS, and the concentrations of propanal, aceticamide (acetamide), isoprene, and 1,3-propanediol are reported to become higher for gastric cancer patients than for normal controls.[49] On the other hand, acetone, isoprene, 1,3-dioxolan-2-one, (toluene), phenol, *m*-xylene, 1,2,3-trimethylbenzene, and phenyl acetate have also been observed in the exhaled gas when using SPI-MS (10.8 eV) and a sampling technique based on thermal adsorption/desorption.[50] Even when using fs-LIMS, it would be difficult to selectively ionize one of the isomers of acetone (*IE* = 9.703 eV, *m/z* = 58) and propanal (*IE* = 9.96 eV, *m/z* = 58) by optimizing the ionization conditions, which is due to small difference in the ionization energies. However, these compounds could be differentiated using a fragment ion observed at *m/z* = 43 for acetone (see Fig. 2) and a fragment ion at *m/z* = 29 for propanal as suggested by the EI-MS database.[37] It would be more difficult to differentiate the isomers of *o*-, *m*-, *p*-xylenes (*IE* = 8.56, 8.55, 8.44 eV),[40] and 1,2,3- and 1,3,5-trimethylbenzenes (*IE* = 8.42, 8.40 eV) since the fragment patterns are very similar among these compounds.[40] However, the intensities of the fragment ions relative to the molecular ions are slightly different from each other even in EI-MS (70 eV) (52, 52, and 58% at *m/z* = 106; 20, 25, and 30% at *m/z* = 105; 100% at *m/z* = 91 for *o*-, *m*-, and *p*-xylenes, and 40 and 70% at *m/z* = 120; and, 100% at *m/z* = 105 for 1,2,3- and 1,3,5-trimethylbenzenes). The distribution of signal intensities could be accurately measured by TOFMS, and the difference in fragment patterns would be more distinctive in fs-LIMS because of the smaller amount of excess energy in the ionic state. Therefore, an evaluation of the contribution of isomers would be more appropriate when conducted using fs-LIMS. Other approaches based on time-delayed measurement and chirp-pulse-ionization mass spectrometry would have a potential for use in differentiation of these isomers.[51-53]

■ CONCLUSIONS

A two-color ionization scheme was utilized in fs-LIMS for trace analysis of the constituents in human exhaled breath. When a combination of the fifth (206 nm) and fourth (257 nm) harmonic emissions was used, the signal intensity of molecular ions was enhanced significantly for acetone via resonance-enhanced, two-photon ionization and the small amount of excess energy remaining in the ionic state. In fact, this technique was employed for the determination of acetone in exhaled breath, permitting the evaluation of obesity and diabetes mellitus online. Numerous chemical species were observed in samples of human exhaled breath, and these could be used to evaluate several health conditions. It is possible to instantly switch the selectivity of fs-LIMS by interrupting one of the beams to optimize the ionization process, which provides additional information concerning the chemical structure of the analytes. Thus, fs-LIMS could be useful for the diagnosis of various diseases such as COVID-19 and cancers in the future.

■ ASSOCIATED CONTENT

Supporting Information

Supporting Information is available free of charge at https://pubs/acs.org/doi/

Optimum wavelength for ionization; photograph of the harmonic generator/combiner; ionization scheme for acetone; mass spectra measured at different wavelengths; mass spectra measured at different laser output powers; dependence of the signal intensity on the laser output power; ionization schemes for N_2, O_2, H_2O, and CO_2; mass spectra of Fig. 2 displayed at a reduced scale; analytical curve measured for acetone; mass spectra of the human breadth measured for the three subjects; expanded views of the mass spectra measured for the human breadth at around m/z = 58; mass spectra measured for the three subjects and the acetone sample prepared at 10 ppm

■ AUTHOR INFORMATION

Corresponding Author

Tomoko Imasaka - *Faculty of Design, Kyushu University, 4-9-1, Shiobaru, Minami-ku, Fukuoka 815-8540: 744 Motooka, Nishi-ku, Fukuoka 819-0395, Japan*; ORCID: 0000-0002-2131-4995; Email: imasaka@design.kyushu-u.ac.jp

Authors

Katsunori Yoshinaga - *Faculty of Design, Kyushu University, 4-9-1, Shiobaru, Minami-ku, Fukuoka 815-8540: 744 Motooka, Nishi-ku, Fukuoka 819-0395, Japan*; ORCID: 0000-0002-9023-2176; Email: yoshinaga.katsunori.407@m.kyushu-u.ac.jp

Totaro Imasaka - *Kyushu University, 744 Motooka, Nishi-ku, Fukuoka 819-0395, Japan Hikari Giken, Co., 2-10-30, Sakurazaka, Chuou-ku, Fukuoka 810-0024, Japan;* ORCID: 0000-0003-4152-3257; Email: TotaroImasaka@gmail.com

Author Contributions

Katsunori Yoshinaga: Measured the standard and real samples reported in this study.
Totaro Imasaka: Supervised the research and wrote the original draft of this paper.
Tomoko Imasaka: Funding acquisition, supervision, computational calculations, and revision of the draft.

Notes

The authors declare no competing financial interest.

■ ACKNOWLEDGMENTS

The authors wish to thank Chen Kuan-Hao and Wu Luo-Xian (undergraduate students) of National Taiwan Normal University for their preliminary studies before starting this work. This research was supported by the AMADA Foundation and the Yanmar Environmental Sustainability Support Association. Quantum chemical calculations were mainly carried out using the computer facilities at the Research Institute for Information Technology, Kyushu University.

■ REFERENCES

(1) The 10th Edition of the Diabetes Atlas compiled by the International Diabetes Federation: https://diabetesatlas.org/atlas/tenth-edition/

(2) Smith, D.; Spanel, P.; Davies, S. Trace gases in breath of healthy volunteers when fasting and after a protein-calorie meal: a preliminary study, *J. Appl. Physiol.* **1999**, *87*, 1584-1588.

(3) Smith, D.; Španěl, P. Selected ion flow tube mass spectrometry (SIFT-MS) for on-line trace gas analysis, *Mass Spectrom. Rev.* **2005**, *24*, 661-700.

(4) Ahead of World Cancer Day, the World Health Organization (WHO)'s cancer agency, the International Agency for Research on Cancer (IARC), Global cancer burden growing, amidst mounting need for services, https://www.who.int/news/item/01-02-2024-global-cancer-burden-growing-amidst-mounting-need-for-services. 1 Feb. 2024.

(5) Hu, B. Mass spectrometric analysis of exhaled breath: Recent advances and future perspectives, *Trends Anal. Chem.* **2023**, *168,* 117320.

(6) Saasa, V.; Malwela, T.; Beukes, M.; Mokgotho, M.; Liu, C. P.; Mwakikunga, B. Sensing technologies for detection of acetone in human breath for diabetes diagnosis and monitoring, *Diagnostics* **2018**, *8*, 12.

(7) Righettoni, M.; Tricoli, A. Toward portable breath acetone analysis for diabetes detection, *J. Breath Res.* **2011**, 5, 037109.

(8) Kim, S.; Park, S.; Park, S.; Lee, C. Acetone sensing of Au and Pd-decorated WO_3 nanorod sensors, *Sens. Actuators B* **2015**, *209*, 180-185.

(9) Yoon, J. W.; Kim, J. S.; Kim, T. H.; Hong, Y. J.; Kang, Y. C.; Lee, J. H. A new strategy for humidity independent oxide chemiresistors: Dynamic self-refreshing of In_2O_3 sensing surface assisted by layer-by-layer coated CeO_2 nanoclusters, *Small* **2016**, *12*, 4229-4240.

(10) Koo, W. T.; Yu, S.; Choi, S. J.; Jang, J. S.; Cheong, J. Y.; Kim, I. D. Nanoscale PdO catalyst functionalized Co_3O_4 hollow nanocages using MOF templates for selective detection of acetone molecules in exhaled breath, *Appl. Mater. Interfaces*

(11) Du, H.; Sun, R.; Su, J.; Sun, Y.; Xia, K.; Cong, L.; Cui, H. Highly selective acetone detector based on a separation channel and semiconductor gas sensor, *Meas. Sci. Technol.* **2021**, *32*, 085102.

(12) Chien, P. J.; Suzuki, T.; Tsujii, M.; Ye, M.; Minami, I.; Toda, K.; Otsuka, H.; Toma, K.; Arakawa, T.; Araki, K.; Iwasaki, Y.; Shinada, K.; Ogawa, Y.; Mitsubayashi, K. Biochemical gas sensors (biosniffers) using forward and reverse reactions of secondary alcohol dehydrogenase for breath isopropanol and acetone as potential volatile biomarkers of diabetes mellitus, *Anal. Chem.* **2017**, *89*, 12261-12268.

(13) Iitani, K.; Chien, P. J.; Suzuki, T.; Toma, K.; Arakawa, T.; Iwasaki, Y.; Mitsubayashi, K. Fiber-optic bio-sniffer (biochemical gas sensor) using reverse reaction of alcohol dehydrogenase for exhaled acetaldehyde, *ACS Sens.* **2018**, *3*, 425-431.

(14) Arakawa, T.; Suzuki, T.; Tsujii, M.; Iitani, K.; Chien, P. J.; Ye, M.; Toma, K.; Iwasaki, Y.; Mitsubayashi, K. Real-time monitoring of skin ethanol gas by a high-sensitivity gas phase biosensor (bio-sniffer) for the non-invasive evaluation of volatile blood compounds, *Biosens. Bioelectron.* **2019**, *129*, 245-253.

(15) Toma, K.; Tsujii, M.; Arakawa, T.; Iwasaki, Y.; Mitsubayashi, K. Dual-target gas-

phase biosensor (bio-sniffer) for assessment of lipid metabolism from breath acetone and isopropanol, *Sens. Actuators B* **2021**, *329*, 129260.
(16) Phillips, M.; Herrera, J.; Krishnan, S.; Zain, M.; Greenberg, J.; Cataneo, R. N. Variation in volatile organic compounds in the breath of normal humans, *J. Chromatogr. B* **1999**, *729*, 75-88.
(17) Deng, C.; Zhang, J.; Yu, X.; Zhang, W.; Zhang, X. Determination of acetone in human breath by gas chromatography-mass spectrometry and solid-phase microextraction with on-fiber derivatization, *J. Chromatogr. B* **2004**, *810*, 269-275.
(18) Rudnicka, J.; Kowalkowski, T.; Ligor, T.; Buszewski, B. Determination of volatile organic compounds as biomarkers of lung cancer by SPME-GC-TOF/MS and chemometrics, *J. Chromatogr. B* **2011**, *879*, 3360-3366.
(19) Ulanowska, A.; Trawińska, E.; Sawrycki, P.; Buszewski, B. Chemotherapy controlled by breath profile with application of SPME-GC/MS method, *J. Sep. Sci.* **2012**, *35*, 2906-2913.
(20) Fishcher, M.; Wohlfahrt, S.; Varga, J.; Matuschek, G.; Saraji-Bozorgzad, M. R.; Denner, T.; Walte, A.; Zimmermann, R. Optically heated ultra-fast-cycling gas chromatography module for separation of direct sampling and online monitoring applications, *Anal. Chem.* **2015**, *87,* 8634-8639.
(21) Mieth, M.; Schubert, J. K.; Gröger, T.; Sabel, B.; Kischkel, S.; Fuchs, P.; Hein, D.; Zimmermann, R; Miekisch, W. Automated needle trap heart-cut GC/MS and needle trap comprehensive two-dimensional GC/TOF-MS for breath gas analysis in the clinical environment, *Anal. Chem.* **2010**, *82,* 2541-2551.
(22) Lindinger, W.; Hansel, A.; Jordan, A. On-line monitoring of volatile organic compounds at pptv levels by means of proton-transfer-reaction mass spectrometry (PTR-MS) Medical applications, food control and environmental research, *Int. J. Mass Spectrom. Ion Processes* **1998**, *173*, 191-241.
(23) Blake, R. S.; Monks, P. S.; Ellis, A. M. Proton-transfer reaction mass spectrometry, *Chem. Rev.* **2009**, *109*, 861-896.
(24) Graus, M.; Müller, M.; Hansel, A. High resolution PTR-TOF: Quantification and formula confirmation of VOC in real time, *J. Am. Soc. Mass Spectrom.* **2010**, *21*, 1037-1044.
(25) Sukul, P.; Trefz, P.; Schubert, J. K.; Miekisch, W. Immediate effects of breath holding maneuvers onto composition of exhaled breath, *J. Breath Res.* **2014**, *8*, 037102.
(26) de Gouw, J.; Warneke, C.; Karl, T.; Eerdekens, G.; van der Veen, C.; Fall, R. Sensitivity and specificity of atmospheric trace gas detection by proton-transfer-reaction mass spectrometry, *Int. J. Mass Spectrom.* **2003**, *223-224*, 365-382.
(27) King, J.; Mochalski, P.; Kupferthaler, A.; Unterkofler, K.; Loc, H.; Filipiak, W.; Teschl, S.; Hinterhuber, H.; Amann, A. Dynamic profiles of volatile organic compounds in exhaled breath as determined by a coupled FTR-MS/GC-MS study, *Physiol. Meas.* **2010**, *31,* 1169-1184.
(28) Righettoni, M.; Schmid, A.; Amann, A.; Pratsinis, S. E. Correlations between blood glucose and breath components from portable gas sensors and PTR-TOF-MS, *J. Breath Res.* **2013**, *7*, 037110.
(29) Španěl, P.; Dryahina, K.; Smith, D. A general method for the calculation of absolute trace gas concentrations in air and breath from selected ion flow tube mass spectrometry data, *Int. J. Mass Spectrom.* **2006**, *249-250*, 230-239.

(30) Mühlberger, F.; Streibel, T.; Wieser, J.; Ulrich, A.; Zimmermann, R. Single photon ionization time-of-flight mass spectrometry with a pulsed electron beam pumped excimer VUV lamp for on-line gas analysis: Setup and first results on cigarette smoke and human breath, *Anal. Chem.* **2005**, *77*, 7408-7414.
(31) Eschner, M. S.; Selmani, I.; Gröger, T. M.; Zimmermann, R. Online comprehensive two-dimensional characterization of puff-by-puff resolved cigarette smoke by hyphenation of fast gas chromatography to single-photon ionization time-of-flight mass spectrometry: Quantification of hazardous volatile organic compounds, *Anal. Chem.* **2011**, *83,* 6619-6627.
(32) Short, L. C.; Frey, R.; Benter, T. Real-time analysis of exhaled breath via resonance-enhanced multiphoton ionization-mass spectrometry with a medium pressure laser ionization source: Observed nitric oxide profile, *Appl. Spectrosc.* **2006**, *60*, 217-222.
(33) Weinkauf, R.; Aicher, P.; Wesley, G.; Grotemeyer, J.; Schlag, E. W. Femtosecond versus nanosecond multiphoton ionization and dissociation of large molecules, *J. Phys. Chem.* **1994**, *98*, 8381-8391.
(34) Matsumoto, J.; Lin, C. H.; Imasaka, T. Supersonic jet multiphoton ionization/mass spectrometry using nanosecond and femtosecond pulse lasers, *Anal. Chim. Acta* **1997**, *343*, 129-133.
(35) Tulej, M.; Ligterink, N. F. W.; de Koning, C.; Grimaudo, V.; Lukmanov, R.; Keresztes Schmidt, P.; Riedo, A.; Wurz, P. Current progress in femtosecond laser ablation/ionisation time-of-flight mass spectrometry. *Appl. Sci.* **2021**, *11*, 2562.
(36) Imasaka, T.; Imasaka, T. Femtosecond ionization mass spectrometry for chromatographic detection, *J. Chromatogr. A* **2021**, *1642*, 462023.
(37) Wen, L.; Yoshinaga, K.; Imasaka, T.; Imasaka, T. Trace analysis of nitrated polycyclic aromatic hydrocarbons based on two-color femtosecond laser ionization mass spectrometry, *Talanta* **2023,** *265*, 124807.
(38) Yoshinaga, K.; Wen, L.; Imasaka, T.; Imasaka, T. Determination of fatty acid methyl esters by two-color two-photon resonance-enhanced femtosecond ionization mass spectrometry, *Anal. Chim. Acta* **2024**, *1296*, 342341.
(39) Yoshinaga, K.; Hao, N. V.; Imasaka, T.; Imasaka, T. Miniature time-of-flight mass analyzer for use in combination with a compact highly-repetitive femtosecond laser ionization source, *Anal. Chim. Acta* **2022**, *1203*, 339673.
(40) NIST Chemistry WebBook: https://webbook.nist.gov/chemistry/
(41) Koch, J. D.; Gronki, J.; Hanson, R. K. Measurements of near-UV absorption spectra of acetone and 3-pentanone at high temperatures, *J. Quant. Spectrosc. Radiat. Transfer* **2008,** *109*, 2037-2044.
(42) Kushch, I.; Arendacká, B.; Štolc, S.; Mochalski, P.; Filipiak, W.; Schwarz, K.; Schwentner, L.; Schmid, A.; Dzien, A.; Lechleitner, M.; Witkovský, V.; Miekisch, W.; Schubert, J.; Unterkofler, K.; Amann, A. Breath isoprene – aspects of normal physiology related to age, gender and cholesterol profile as determined in a proton transfer reaction mass spectrometry study, *Clin. Chem. Lab. Med.* **2008**, *46*, 1011-1018.
(43) King, J.; Kupferthaler, A.; Unterkofler, K.; Koc, H.; Teschl, S.; Teschl, G.; Miekisch, W.; Schubert, J.; Hinterhuber, H.; Amann, A. Isoprene and acetone concentration profiles during exercise on an ergometer, *J. Breath Res.* **2009**, *3*, 027006.

(44) Portillo-Estrada, M.; Van Moorleghem, C.; Janssenswillen, S.; Cooper, R. J.; Birkemeyer, C.; Roelants, K.; Van Damme, R. Proton-transfer-reaction time-of-flight mass spectrometry (PTR-TOF-MS) as a tool for studying animal volatile organic compound (VOC) emissions, *Methods Ecol. Evol.* **2021**, *12*, 748-766.
(45) Kleeblatt, J.; Schubert, J. K.; Zimmermann, R. Detection of gaseous compounds by needle trap sampling and direct thermal-desorption photoionization mass spectrometry: Concept and demonstrative application to breath gas analysis, *Anal. Chem.* **2015**, *87*, 1773-1781.
(46) Tanaka, M.; Matsui, T. Identification of characteristic compounds of moderate volatility in breast cancer cell lines. *PLoS One* **2020**, *15*, e0235442.
(47) Liangou, A.; Tasoglou, A.; Huber, H. J.; Wistrom, C.; Brody, K.; Menon, P. G.; Bebekoski, T.; Menschel, K.; Davidson-Fiedler, M.; DeMarco, K.; Salphale, H.; Wistrom, J.; Wistrom, S.; Lee, R. J. A method for the identification of COVID-19 biomarkers in human breath using Proton Transfer Reaction Time-of-Flight Mass Spectrometry, *eClinicaMedicine* **2021**, *42*, 101207.
(48) Traxler, S.; Barkowsky, G.; Saß, R.; Klemenz, A. C.; Patenge, N.; Kreikemeyer, B.; Schubert, J. K.; Miekisch, W. Volatile scents of influenza A and S. pyogenes (co-)infected cells, *Sci. Rep.* **2019**, *9*, 18894.
(49) Jung, Y. J.; Seo, H. S.; Kim, J. H.; Song, K. Y.; Park, C. H.; Lee, H. H. Advanced diagnostic technology of volatile organic compounds real time analysis from exhaled breath of gastric cancer patients using proton-transfer-reaction time-of-flight mass spectrometry, *Front. Oncol.* **2021**, *11*, 560591.
(50) Hong, Y.; Che, X.; Su, H.; Mai, Z.; Huang, Z.; Huang, W.; Chen, W.; Liu, S.; Gao, W.; Zhou, Z.; Tan, G.; Li, X. Exhaled breath analysis using on-line preconcentration mass spectrometry for gastric cancer diagnosis, *J. Mass Spectrom.* **2021**, *56*, e4588.
(51) McPherson, S. L.; Shusterman, J. M.; López Peña, H. A. Boateng, D. A.; Tibbetts, K. M. Quantitative analysis of nitrotoluene isomer mixtures using femtosecond time-resolved mass spectrometry, *Anal. Chem.* **2021**, *93*, 11268−11274.
(52) Stamm, J.; DeJesus, L.; Jones, A. D.; Dantus, M. Quantitative identification of nonpolar perfluoroalkyl substances by mass spectrometry, *J. Phys. Chem. A* **2022**, *126*, 8851−8858.
(53) Schäfer, V.; Weitzel, K. M. Qualitative and quantitative distinction of *ortho*-, *meta*-, and *para*-fluorotoluene by means of chirped femtosecond laser ionization, *Anal. Chem.* **2020**, *92*, 5492−5499.

Figure Captions

Fig. 1 Block diagram of the experimental apparatus.

Fig.2 Mass spectra measured for (A) acetone (10 ppm) diluted with pure air (B) no acetone. M^+, molecular ion; F^+, fragment ion. Ionization source; 62 mW at 257 nm and 20 mW at 206 nm. Assignment: 7, N^{2+}; 8, O^{2+}; 14, N^+; 16, O^+; 18, $^{18}O^+$ and H_2O^+; 28, N_2^+; 32, O_2^+; 34, $^{16}O^{18}O^+$; 43, CH_3CO^+ (acetone, fragment ion); 57, $CH_3COCH_2^+$ (acetone, fragment ion); 58, $CH_3COCH_3^+$ (acetone, molecular ion); 59, $^{12}C_2{}^{13}COH_6^+$ (acetone, isotopomer ion). Locations of the molecular ion (*m/z* = 58) and the fragment ions (*m/z* = 43) are indicated by arrows in (B).

Fig. 3 Mass spectra measured for (A) exhaled breath (B) room air in the laboratory. Ionization source; 62 mW at 257 nm and 19 mW at 206 nm. Assignment: 39, $C_3H_3^+$ (isoprene fragment); 40, $C_3H_4^+$ (isoprene fragment); 41, $C_3H_5^+$ (isoprene fragment), 44, CH_3CHO^+ (acetaldehyde, molecular ion); 46, $CH_3CH_2OH^+$ (ethanol, molecular ion); 53, $CH_2=C^+-CH=CH_2$ (isoprene, fragment ion); 67, $CH_2=C(CH_3)CH=CH^+$ (isoprene, fragment ion); 68, $CH_2=C(CH_3)CH=CH_2^+$ (isoprene, molecular ion); 69, $^{12}C_4{}^{13}CH_8^+$ (isoprene, isotopomer ion). Locations of the molecular ion, $[M]^+$ (*m/z* = 58), and the fragment ions, $[F]^+$ (*m/z* = 43), are indicated by arrows in the figure.

Fig. 4 Mass spectrum measured for human exhaled breath. Ionization source; 62 mW at 257 nm and 19 mW at 206 nm. Possible assignments are indicated in the figure. BG, background signal arising from the mass spectrometer.

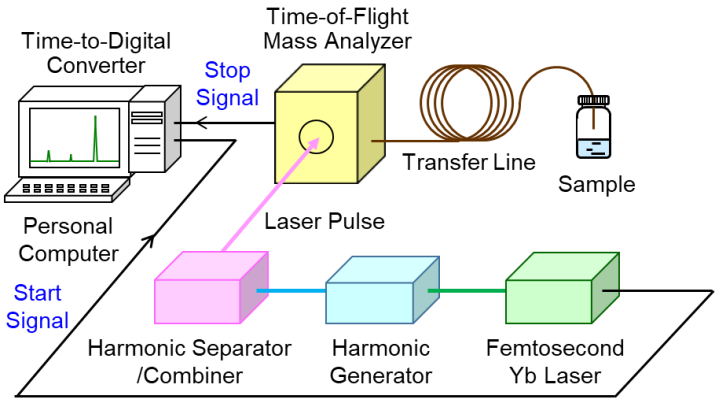

Figure 1 K. Yoshinaga, et al.

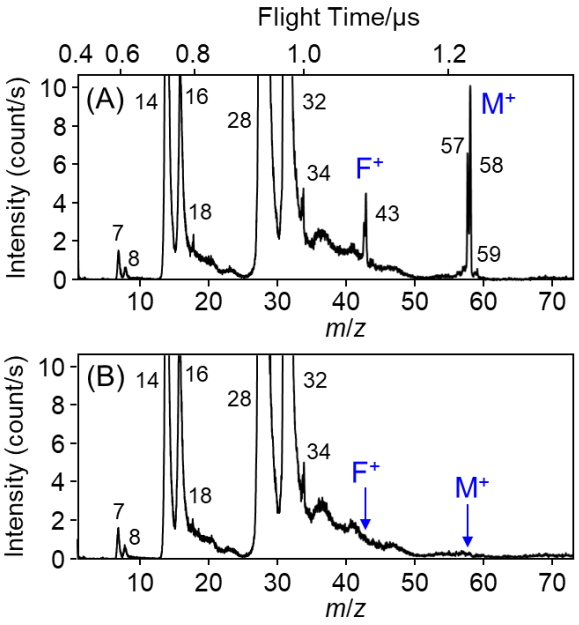

Figure 2 K. Yoshinaga, et al.

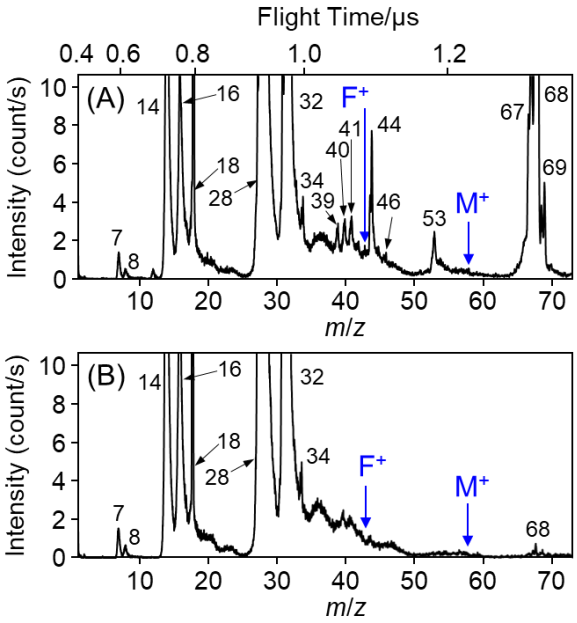

Figure 3 K. Yoshinaga, et al.

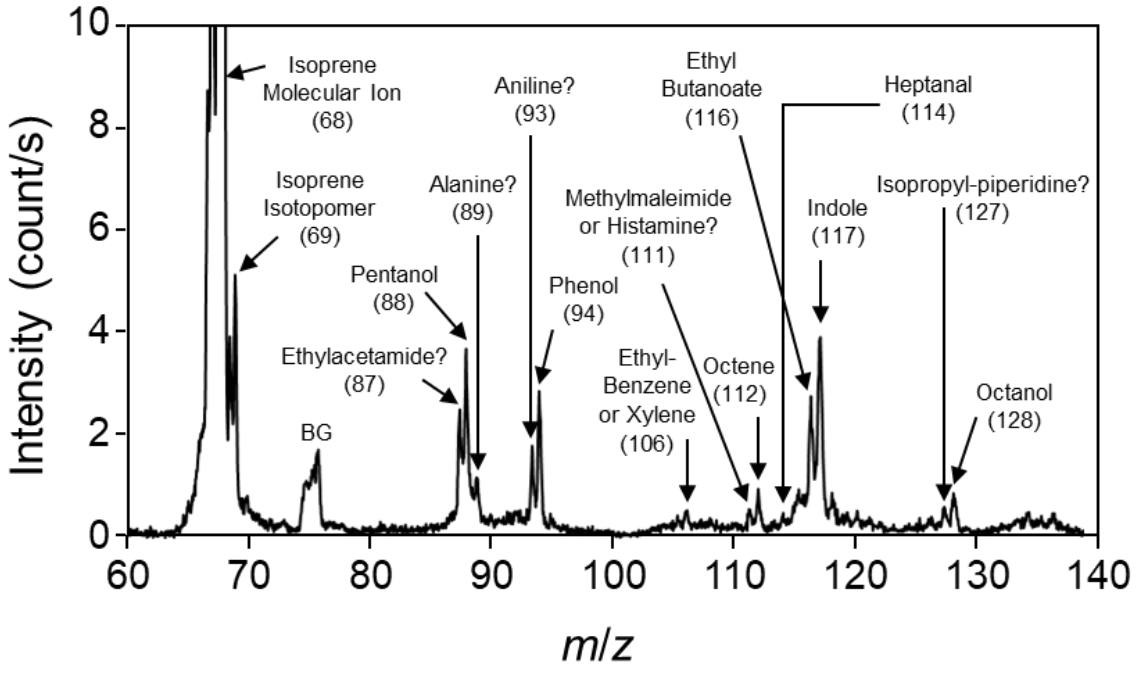

Figure 4 K. Yoshinaga, et al.

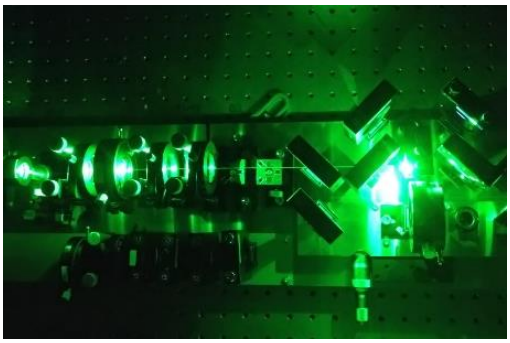

TOC

Supporting information

Femtosecond Laser Ionization Mass Spectrometry for Online Analysis of Human Exhaled Breath

Katsunori Yoshinaga,[a] Totaro Imasaka,[b,c] Tomoko Imasaka[a]*

[a]*Faculty of Design, Kyushu University, 4-9-1, Shiobaru, Minami-ku, Fukuoka 815-8540: 744 Motooka, Nishi-ku, Fukuoka 819-0395, Japan*
[b]*Kyushu University, 744 Motooka, Nishi-ku, Fukuoka 819-0395, Japan*
[c]*Hikari Giken, Co., 2-10-30, Sakurazaka, Chuou-ku, Fukuoka 810-0024, Japan*

Table of Contents

Text

Optimal wavelength for ionization

The mass spectrum measured at 257 nm appears in Fig. S3(A). In the NIST database obtained using EI-MS, the intensity of the molecular ion observed at *m/z* = 58 is 25% of the base peak at *m/z* = 43. Therefore, the molecular ion could be enhanced significantly by fsLI-MS. To examine the ionization process, a mass spectrum was measured at different laser output powers (the mass spectra are shown in Fig. S4, and the dependence of the signal intensity of the fragment ion at *m/z* = 43 on the laser output power appears in Fig. S5). The slope of the observed data was 2.4, suggesting that three photons are necessary for ionization (see Fig. S3(A)).

The mass spectrum measured at 206 nm appears in Fig. S3(B). The molecular ion was slightly enhanced when compared with the data obtained at 257 nm. This favorable result was observed when using two-photon ionization that is more efficient than three-photon ionization (see Fig. S2(B)), and this resulted in a smaller amount of excess energy (2.33 eV) remaining in the ionic state. However, the enhancement of the molecular ion was minimal, since the excess energy was sufficient for the dissociation of a CH_3-group. Moreover, the signal intensities were decreased appreciably due to the smaller level of output power at 206 nm.

The mass spectrum measured by two-color, two-photon ionization at 257 and 206 nm is shown in Fig. S3(C). The molecular ion was drastically enhanced when using this ionization scheme, and the fragmentation was suppressed by decreasing the excess energy (1.13 eV). In fact, the signal intensity increased significantly because of the large output power of the optical pulse at 257 nm. Thus, a scheme of two-color, two-photon ionization (see Fig. S2(C)) provides a useful means for a sensitive, as well as selective, determination of acetone.

Figures

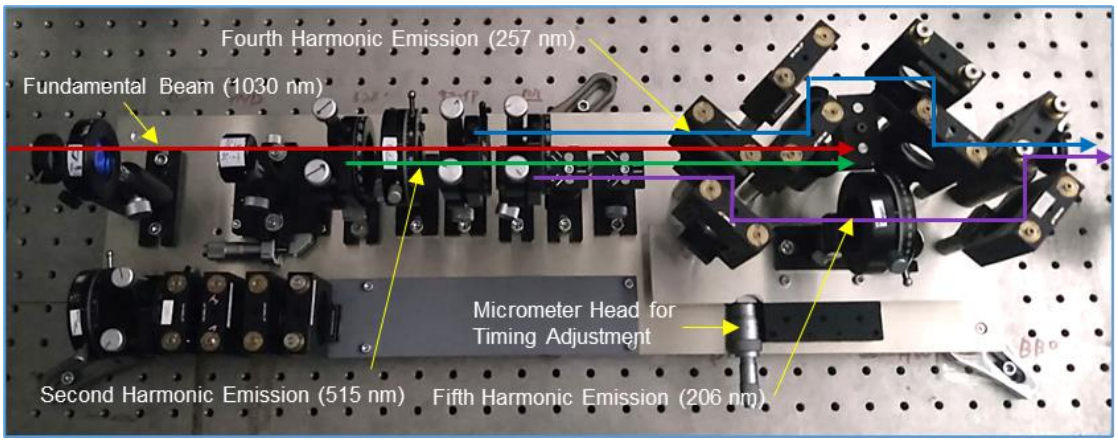

Figure S1. Photograph of the harmonic generator/combiner.

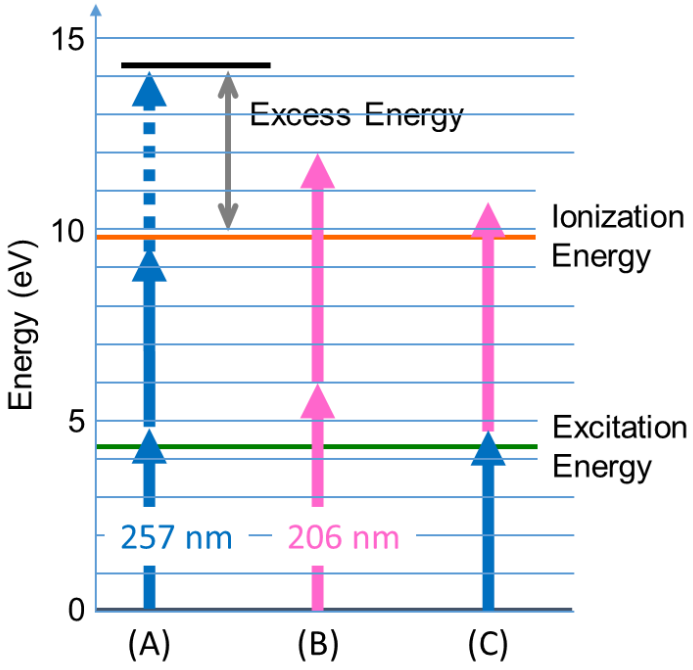

Figure S2. Ionization scheme of acetone. (A) single-color three-photon ionization at 257 nm (B) single-color two-photon ionization at 206 nm (C) two-color two-photon ionization at 257 and 206 nm.

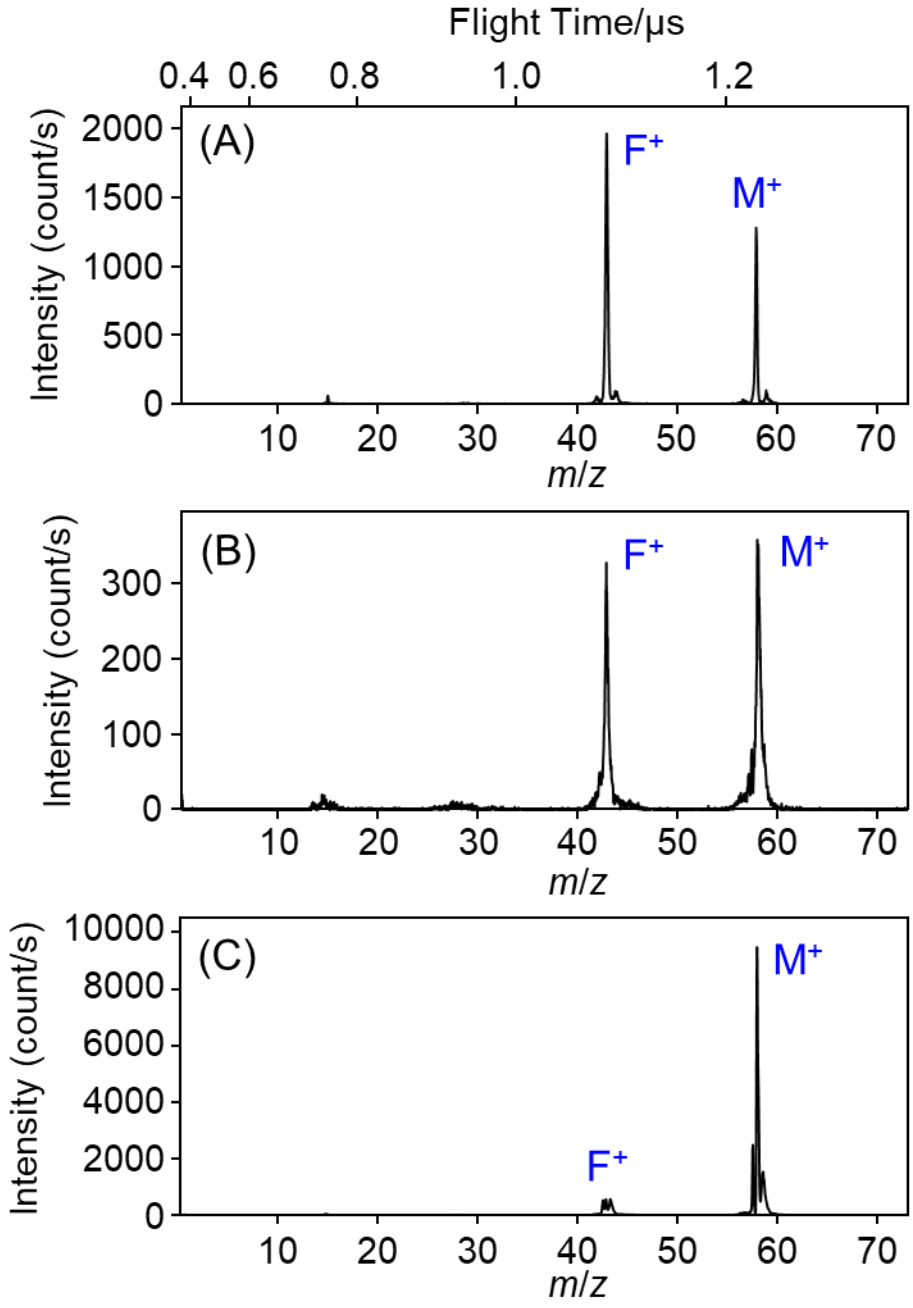

Figure S3. Mass spectra measured at (A) 257 nm (57 mW) (B) 206 nm (17 mW) (C) 257 nm (57 mW) + 206 nm (17 mW). M^+, molecular ion; F^+, fragment ion. The acetone in a GC vial was vaporized continuously and was introduced into the mass spectrometer.

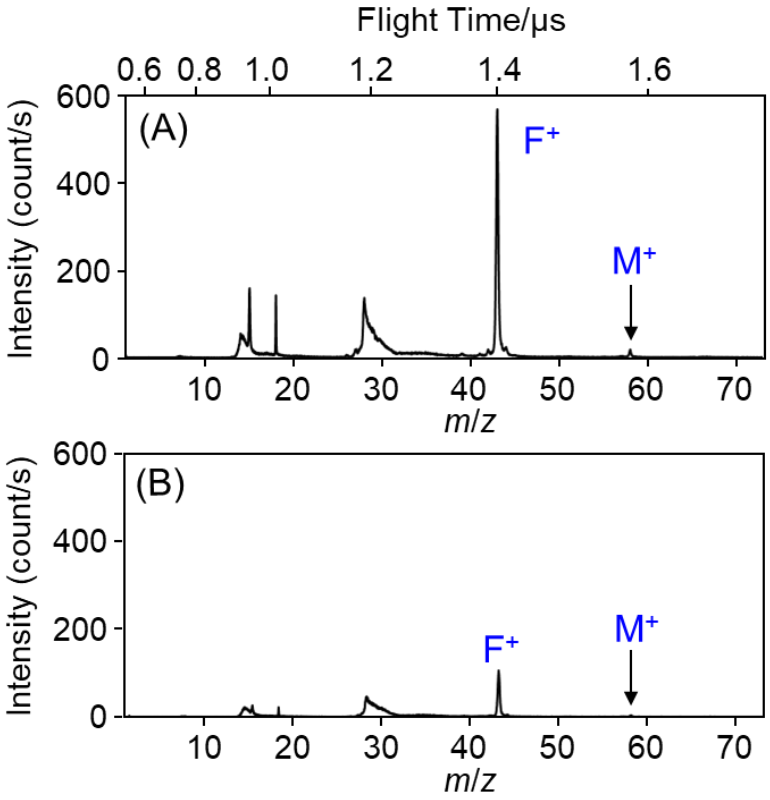

Figure S4. Mass spectra measured at (A) 200 mW (B) 100 mW. Concentration of acetone, 150 ppm. Ionization wavelength, 257 nm.

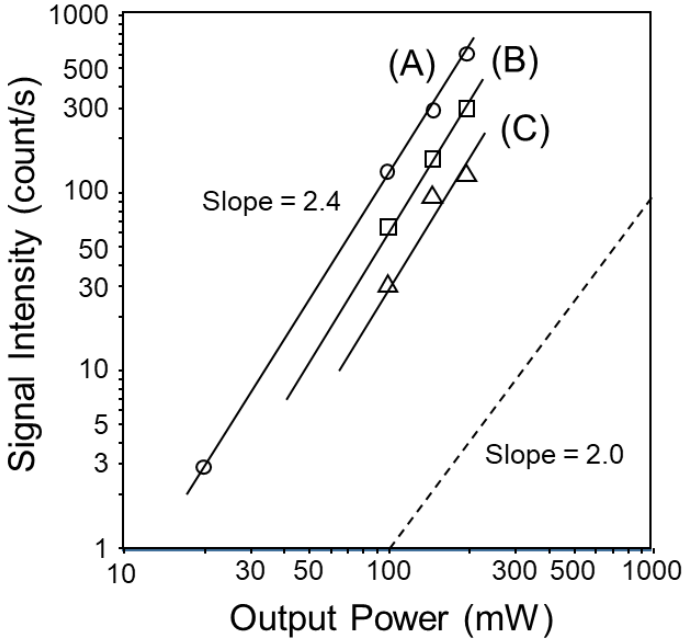

Figure S5. Dependence of the signal intensity of the fragment ion at *m/z* = 43 on the laser output power. Concentration of acetone, (A)150 ppm (B) 100 ppm (C) 50 ppm. Broken line (slope = 2.0)

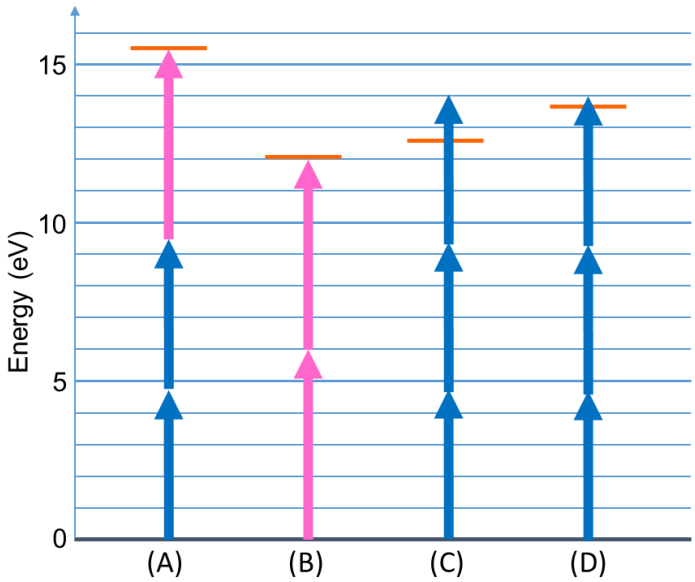

Figure S6. Ionization schemes. (A) N_2, *IE* = 15.581 eV (B) O_2, *IE* = 12.070 eV (C) H_2O, *IE* = 12.621 eV (D) CO_2, *IE* = 13.777 eV (the data are cited from the NIST database).

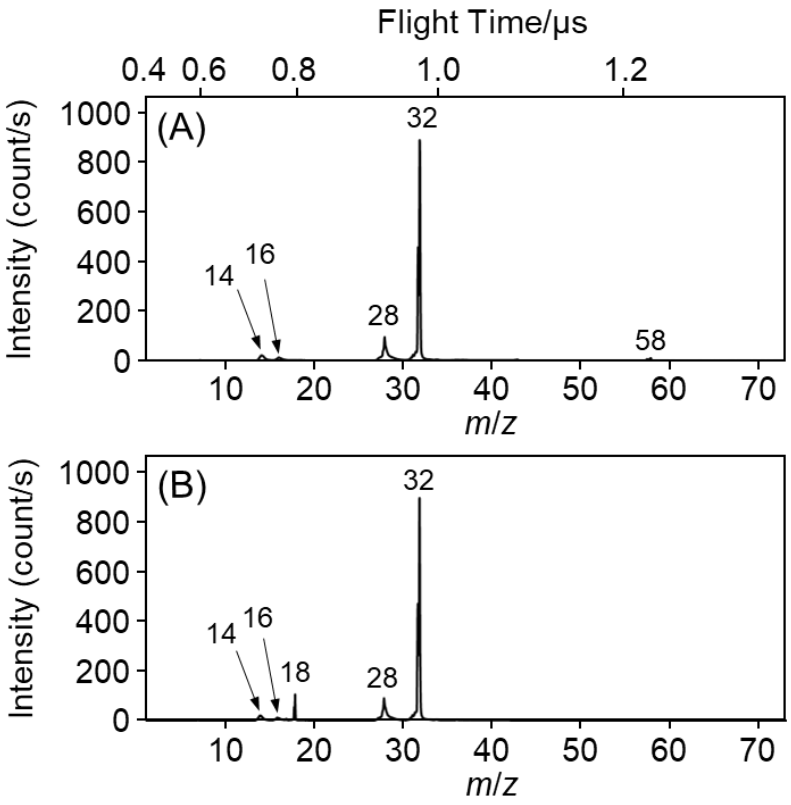

Figure S7. Mass spectra measured for (A) acetone (10 ppm) diluted with pure air (B) no acetone. The data obtained in Fig. 2 are displayed at a reduced scale.

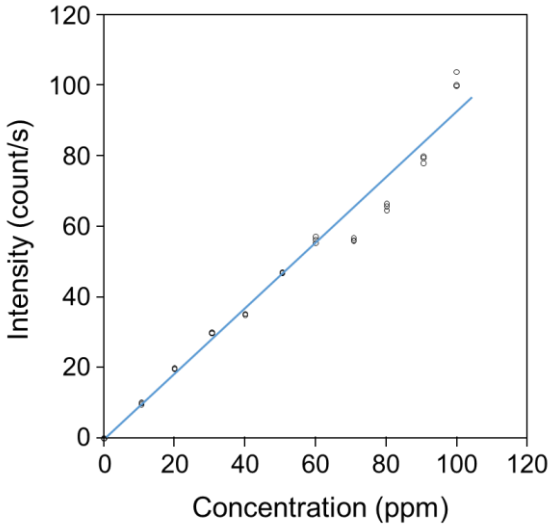

Figure S8. Analytical curve measured for acetone diluted with the pure air in a cylinder. The data were observed three time at each concentration. The deviation of the data from a linear curve was not arising from the inaccuracy in the measurement but from the error in reading the flow rate of the air in the standard gas generator, since the standard deviation of the signal intensity was smaller than the deviation from the analytical curve. It is noted that the reading error increases at lower flow rates of the air to prepare the acetone gas at high concentrations. This issue can be solved by replacing the analog flow meter with a digital mass flow controller with better accuracy.

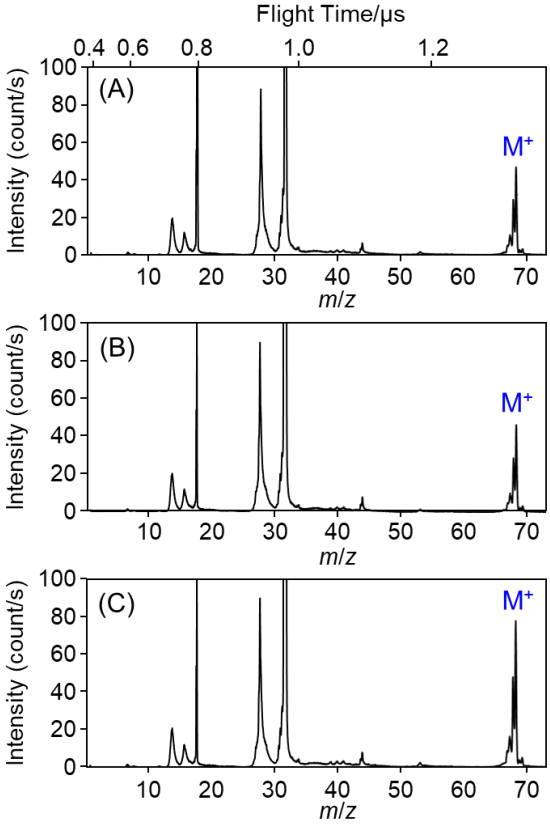

Figure S9. Mass spectra of the human breadth from the three subjects (A), (B), (C). M^+ is the molecular ion of isoprene. The signal peak at m/z = 28 can be assigned to N_2^+ arising from N_2 in the exhaled breath, indicating excellent repeatability in fs-LIMS.

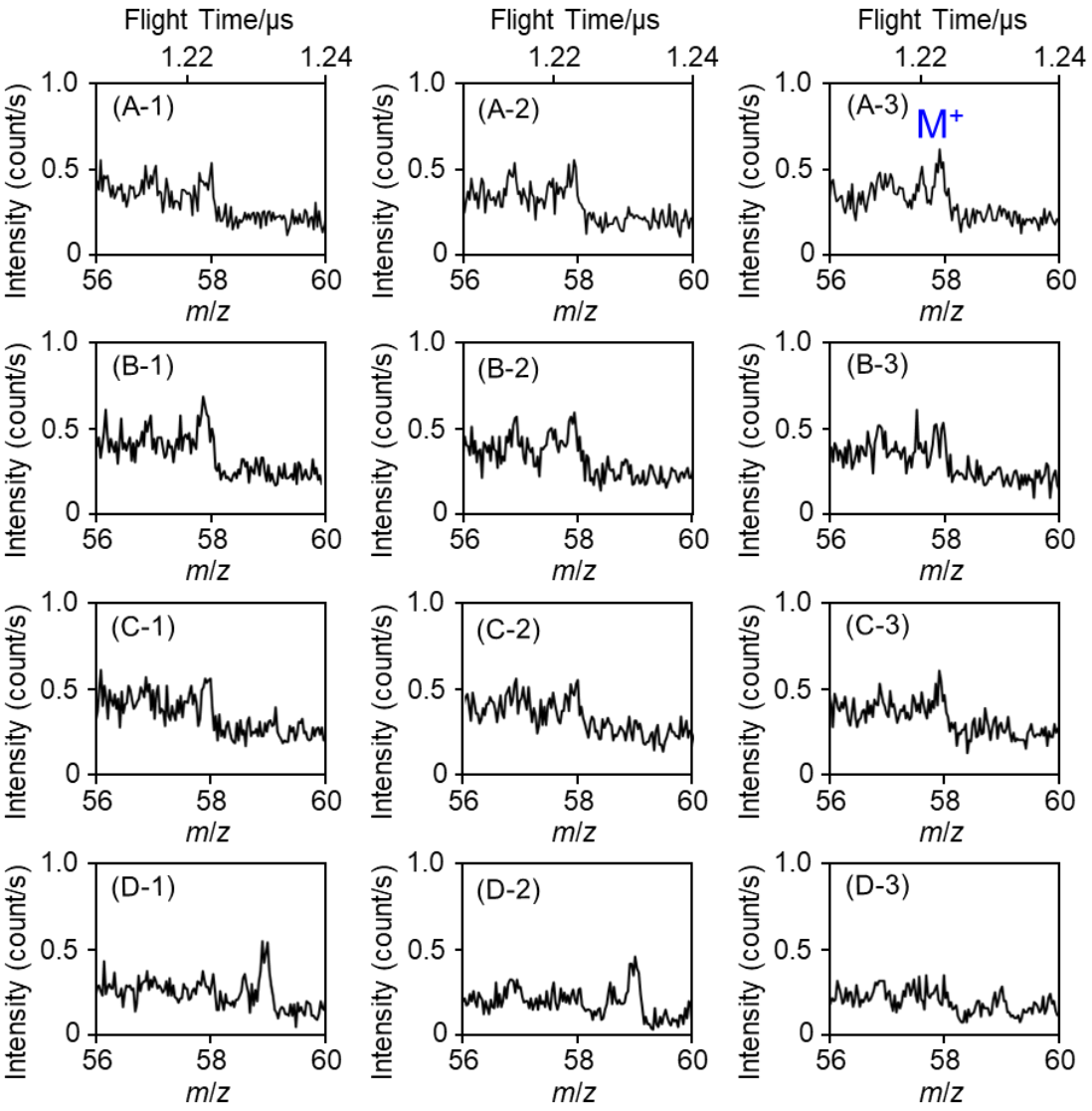

Figure S10. Triplicated mass spectra of the human breadth from the three subjects (A) (B) (C). The concentration of acetone was calculated to be (A) 0.30 ± 0.03 ppm (B) 0.34 ± 0.04 ppm (C) 0.30 ± 0.02 ppm, respectively. (D) the background spectrum measured for a room air.

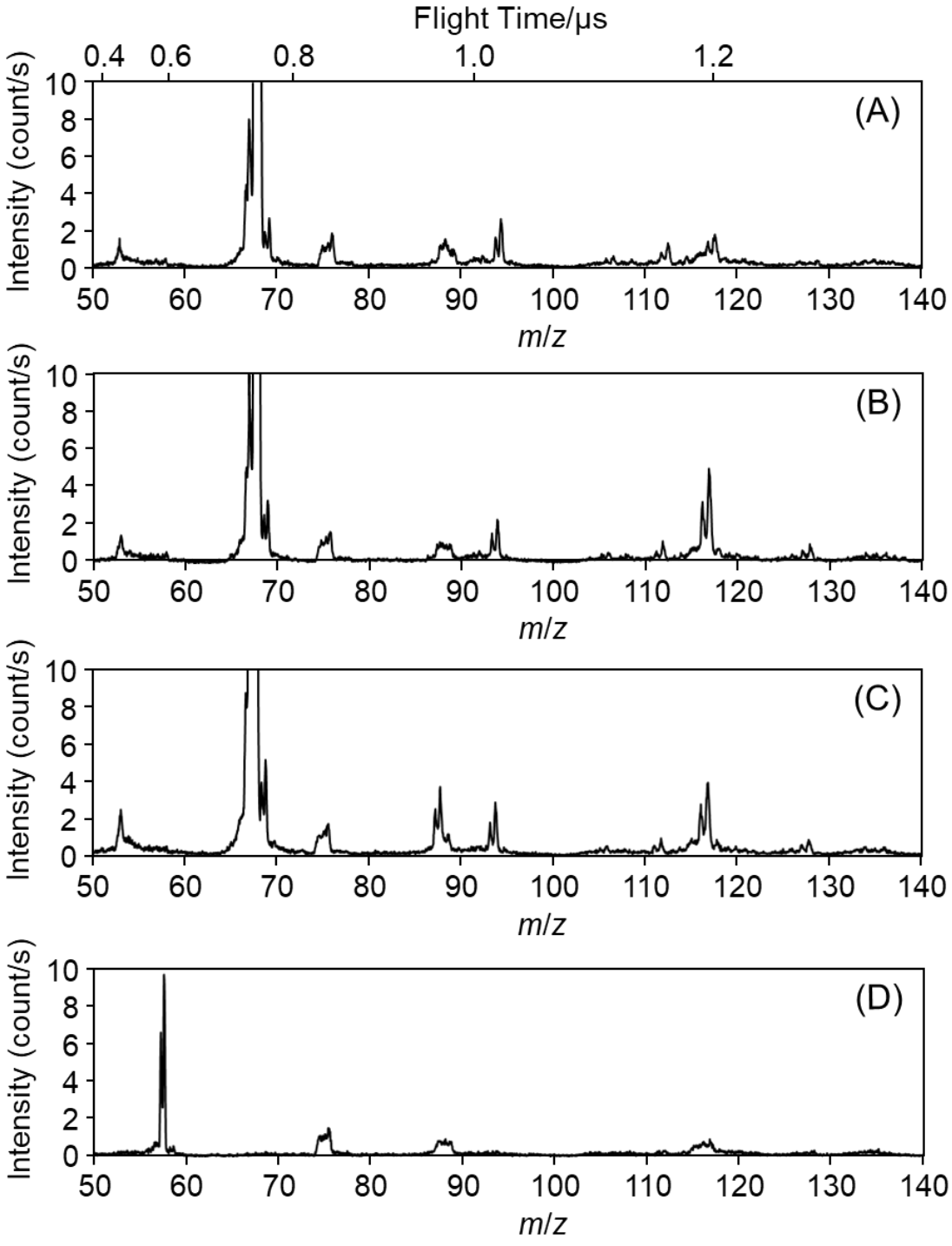

Figure S11. Mass spectra measured for (A) (B) (C) three subjects and (D) acetone prepared at 10 ppm using the pure air in a cylinder.